

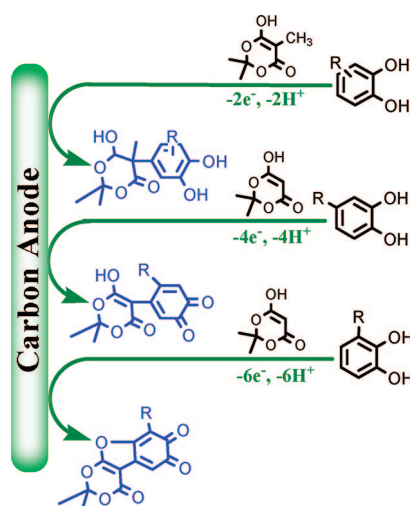
# Kinetic Study of Electrochemically Induced Michael Reactions of *o*-Quinones with Meldrum's Acid Derivatives. Synthesis of Highly Oxygenated Catechols

D. Nematollahi\* and H. Shayani-jam

Faculty of Chemistry, University of Bu-Ali-Sina, Hamadan, 65174, Iran

nemat@basu.ac.ir

Received January 17, 2008



Electrochemical oxidation of catechols has been studied in the presence of Meldrum's acid derivatives as nucleophiles in aqueous solution, by means of cyclic voltammetry and controlled-potential coulometry. Catechols in the Michael addition reaction react with Meldrum's acids to form adducts that can undergo electrooxidation. Such products were obtained in good yields as confirmed by controlled potential electrosynthesis. Such products can be generated in aqueous solutions by means of electrosynthesis, using a carbon electrode in an undivided cell. Furthermore, the homogeneous rate constants of the chemical reaction interposed between electron transfers were estimated by comparing the experimental cyclic voltammetric curves with the digitally simulated ones.

## Introduction

Investigation of catechol derivatives may lead to the discovery of selectively acting, biodegradable agrochemicals with a human, animal, and plant compatibility.<sup>1,2</sup> One of the most important groups of catechols are catecholamines. Catecholamines are compounds containing a catechol nucleus and amine group on a chain of two carbon atoms meta or para to the phenolic hydroxyl groups and are bioenergetic amines that play quite an important role as neurotransmitters in the central nervous system

(CNS). And accordingly, their electrochemistry has been investigated extensively.<sup>3</sup> Furthermore, *o*-quinones are of considerable interest because many drugs such as doxorubicin, daunorubicin, and mitomycin C in cancer chemotherapy contain quinones,<sup>4</sup> whereas various other quinones have found use in industry.<sup>5</sup> Some of them also exhibit antitumor and antimalarial activities<sup>6</sup> and many of them are also involved in enzyme inhibition and DNA cross-linking.<sup>7</sup> Also, it is demonstrated in comparison with simple catechols and quinones that highly oxygenated catechols<sup>8,9</sup> and quinones<sup>10</sup> exhibit interesting biological activities. After the valuable published paper on the electrochemical oxidation of substituted catechols by Ryan et al. in 1980,<sup>11</sup> in recent years we and others have investigated the electrochemical oxidation of some catechols in the presence

\* Corresponding author. Fax: 0098-811-8272404, Phone: 0098-811-8271541.

(1) AMiCBASE-EssOil, *Database on Natural Antimicrobials*; Review Science: Germany (1999–2002).

(2) Pauli, A. *Antimicrobial Properties of Catechol Derivatives*; Proceeding of the 3rd World Congress on Allelopathy: Tsukuba, Japan, August, 2002.

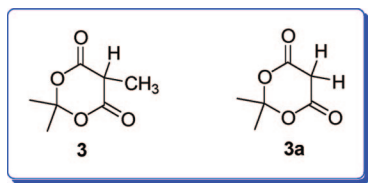


**FIGURE 1.** The structures of methyl-Meldrum's acid (**3**) and Meldrum's acid (**3a**).

of nucleophiles for obtaining new catechols and quinone derivatives.<sup>12–22</sup> But the development of a simple synthetic route for the synthesis of highly oxygenated catechols and quinones from readily available reagents is one of the major tasks in this paper. This idea prompted us to investigate the electrochemical oxidation of catechols in the presence of Meldrum's acid derivatives as nucleophiles (Figure 1) and represents a facile and one-pot electrochemical method for the synthesis of some new highly oxygenated catechols and quinones. Also, an additional purpose of this work is the kinetic and mechanistic study of the electrochemical oxidation of catechols in the presence of Meldrum's acid derivatives and the estimation of the observed homogeneous rate constants ( $k_{\text{obs}}$ ) of reaction of electrochemically generated *o*-benzoquinones with these nucleophiles by digital simulation of cyclic voltammograms.

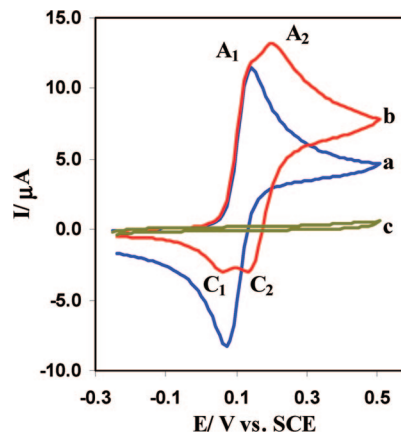


**FIGURE 2.** Cyclic voltammograms of (a) 1.0 mM 3-methylcatechol in the absence of methyl-Meldrum's acid, (b) in the presence of 1.0 mM methyl-Meldrum's acid, and (c) 1.0 mM methyl-Meldrum's acid in the absence of 3-methylcatechol at a glassy carbon electrode, in phosphate buffer solution (pH 7.0,  $c = 0.2$  M). Scan rate:  $100 \text{ mV s}^{-1}$ .  $t = 25^\circ \text{C}$ .

## Results and Discussion

**Electrochemical Oxidation of Catechols in the Presence of Methyl-Meldrum's Acid.** Figure 2 (curve a) shows a cyclic voltammogram recorded for 1.0 mM 3-methylcatechol (**1a**) in aqueous solution containing 0.2 M phosphate buffer (pH 7.0). The voltammogram shows an anodic peak ( $A_1$ ) in the positive-going scan and a cathodic counterpart peak ( $C_1$ ) in the negative-going scan, which corresponds to the transformation of 3-methylcatechol (**1a**) to *o*-benzoquinone **2a** and vice versa within a quasireversible two-electron process.<sup>11–20,23</sup> In basic solutions, the peak current ratio ( $I_{\text{pC1}}/I_{\text{pA1}}$ ) is less than unity and decreases with increasing pH as well as by decreasing the potential sweep rate. These can be related to the coupling of anionic or dianionic forms of catechols with *o*-benzoquinones (dimerization reaction).<sup>11,23,24</sup>

The oxidation of 3-methylcatechol (**1a**) in the presence of methyl-Meldrum's acid (**3**) as a nucleophile was studied in some detail. Figure 2 (curves b) shows the cyclic voltammogram obtained for a 1.0 mM solution of **1a** in the presence of methyl-Meldrum's acid (**3**) in aqueous solution containing 0.2 M phosphate buffer (pH 7.0). In this condition, the voltammogram exhibits two anodic peaks  $A_1$  and  $A_2$  (at more positive potentials) and two cathodic related peaks ( $C_1$  and  $C_2$ ).

The existence of a subsequent chemical reaction is supported by the following evidence: (a) During the reverse scan, the peak corresponding to the reduction of the *o*-benzoquinone **2a** decreases (Figure 2). This could be indicative of the fact that *o*-benzoquinone **2a** formed at the surface of an electrode is removed by chemical reaction with methyl-Meldrum's acid (**3**). (b) Figure 3 presents the variation of the oxidation peak current of **1a** ( $A_1$  and  $A_2$ ) versus the potential scan rate in the presence of **3**. It is seen that proportional to the augmentation of potential sweep rate, parallel to the increase in height of the  $C_1$ , the height of  $C_2$  decreases. A plot of the peak current ratio ( $I_{\text{pC1}}/I_{\text{pA1}}$ ) versus scan rate for a mixture of **1a** and methyl-Meldrum's acid (**3**) confirms the reactivity of **2a** toward methyl-Meldrum's acid (**3**), appearing as an increase in the peak current ratio ( $I_{\text{pC1}}/I_{\text{pA1}}$ ) at higher scan rates. Also, the current function for peak  $A_1$ , ( $I_{\text{pA1}}/$

(3) (a) Sabeti, J.; Gerhardt, G. A.; Zahniser, N. R. *Neurosci. Lett.* **2003**, *343*, 9. (b) Reed, B.; Chen, N.; Justice, J. B. *J. Neurosci. Methods* **2003**, *126*, 127. (c) Greco, P. G.; Garris, P. A. *Eur. J. Pharmacol.* **2003**, *479*, 117. (d) Whitley, J.; Parsons, J.; Freeman, J.; Liu, Y.; Edwards, R. H.; Near, J. A. *J. Neurosci. Methods* **2004**, *133*, 191. (e) Mateo, Y.; Budygin, E. A.; John, C. E.; Banks, M. L.; Jones, S. R. *J. Neurosci. Methods* **2004**, *140*, 183. (f) Crespi, F.; Dalessandro, D.; Annovazzi-Lodi, V.; Heidebreder, C.; Norgia, M. *J. Neurosci. Methods* **2004**, *140*, 153. (g) Garris, P. A.; Ensman, R.; Poehlman, J.; Alexander, A.; Langley, P. E.; Sandberg, S. G.; Greco, P. G.; Wightman, R. M.; Rebec, G. V. *J. Neurosci. Methods* **2004**, *140*, 103. (h) Schenk, J. O.; Wright, C.; Bjorklund, N. *J. Neurosci. Methods* **2005**, *143*, 41. (i) Borland, L. M.; Shi, G.; Yang, H.; Michael, A. C. *J. Neurosci. Methods* **2005**, *146*, 149. (j) Greco, P. G.; Meisel, R. L.; Heidenreich, B. A.; Garris, P. A. *J. Neurosci. Methods* **2006**, *152*, 55. (k) Volz, T. J.; Hanson, G. R.; Fleckenstein, A. E. *J. Neurosci. Methods* **2006**, *155*, 109. (l) Bergstrom, B. P.; Cummings, D. R.; Skaggs, T. A. *Neuropharmacology* **2007**, *53*, 967. (m) Kagohashi, M.; Nakazato, T.; Yoshimi, K.; Moizumi, S.; Hattori, N.; Kitazawa, S. *Neurosci. Res.* **2008**, *60*, 120. (n) Afkhami, A.; Nematollahi, D.; Khalafi, L.; Rafiee, M. *Int. J. Chem. Kinet.* **2005**, *37*, 17. (o) Afkhami, A.; Nematollahi, D.; Madrakian, T.; Khalafi, L. *Electrochim. Acta* **2005**, *50*, 5633.

(4) Blum, R. H.; Carter, S. K. *Ann. Intern. Med.* **1974**, *80*, 249. (5) Kaleem, K.; Chertok, F.; Erhan, S. *Prog. Org. Coating* **1987**, *15*, 63. (6) Huang, Z. D.; Chen, Y. N.; Menon, K.; Teicher, B. A. *J. Med. Chem.* **1993**, *36*, 1797. (7) Bittner, S.; Meenakshi, C.; Temtsin, G. *Tetrahedron* **2001**, *57*, 7423. (8) Sawayama, Y.; Tsujimoto, T.; Sugino, K.; Nishikawa, T.; Isobe, M.; Kawagishi, H. *Biosci. Biotechnol. Biochem.* **2006**, *70*, 2998. (9) Bui, V. P.; Hansen, T. V.; Stenstrom, Y.; Hudlicky, T. *Green Chem.* **2000**, *2*, 263. (10) Dalton, R. D. *The Alkaloids*; Academic Press: New York, 1979; p 264. (11) Ryan, M. D.; Ueh, A. Y.; Wen-Yu, C. *J. Electrochem. Soc.* **1980**, *127*, 1489. (12) Nematollahi, D.; Alimoradi, M.; Rafiee, M. *J. Phys. Org. Chem.* **2007**, *20*, 49. (13) Shamsipur, M.; Hosseiny Davarani, S. S.; Nasiri-Aghdam, M.; Nematollahi, D. *Electrochim. Acta* **2006**, *51*, 3327. (14) Nematollahi, D.; Alimoradi, M.; Waqif Husain, S. *Electrochim. Acta* **2006**, *51*, 2620. (15) Nematollahi, D.; Tammari, E. *J. Org. Chem.* **2005**, *70*, 7769. (16) Nematollahi, D.; Rahchamani, R. *Tetrahedron Lett.* **2002**, *43*, 147. (17) Nematollahi, D.; Hesari, M. *J. Electroanal. Chem.* **2005**, *577*, 197. (18) Nematollahi, D.; Habibi, D.; Rahmati, M.; Rafiee, M. *J. Org. Chem.* **2004**, *69*, 2637. (19) Nematollahi, D.; Golabi, S. M. *J. Electroanal. Chem.* **1996**, *405*, 133. (20) Habibi, D.; Nematollahi, D.; Seyyed Al-Hoseini, Z.; Dehdashtian, S. *Electrochim. Acta* **2006**, *52*, 1234. (21) Findley, T. K. Quinones as Synthons. In *The chemistry of quinonoid compounds*; Patai, S., Rappoport, Z., Eds.; John Wiley & Sons: Chichester, UK, 1988; Vol. 2, Part 1. (22) Chambers, J. Q. In *Electrochemistry of quinones*. In *The Chemistry of Quinonoid Compounds*; Patai, S., Rappoport, Z., Eds.; John Wiley & Sons: Chichester, UK, 1988.

(23) Nematollahi, D.; Rafiee, M. *J. Electroanal. Chem.* **2004**, *566*, 31.

(24) Nematollahi, D.; Rafiee, M.; Samadi-Maybodi, A. *Electrochim. Acta* **2004**, *49*, 2495.

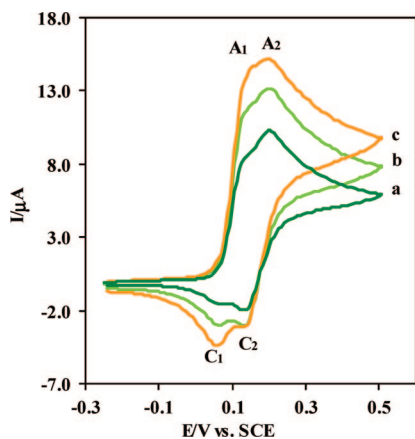


**FIGURE 3.** Typical cyclic voltammograms of 1.0 mM 3-methylcatechol in the presence of 1.0 mM methyl-Meldrum's acid at a glassy carbon electrode, in phosphate buffer solution (pH 7.0, 0.2 M). Scan rates from curves a–c are 25, 50, and 100  $\text{mV s}^{-1}$ , respectively.  $t = 25^\circ\text{C}$ .

$v^{1/2}$ ), decreases slightly with increasing the scan rate. (c) The intensity of the oxidation peak A<sub>2</sub> (and its counterpart) increases as the concentration of methyl-Meldrum's acid (**3**) increases.

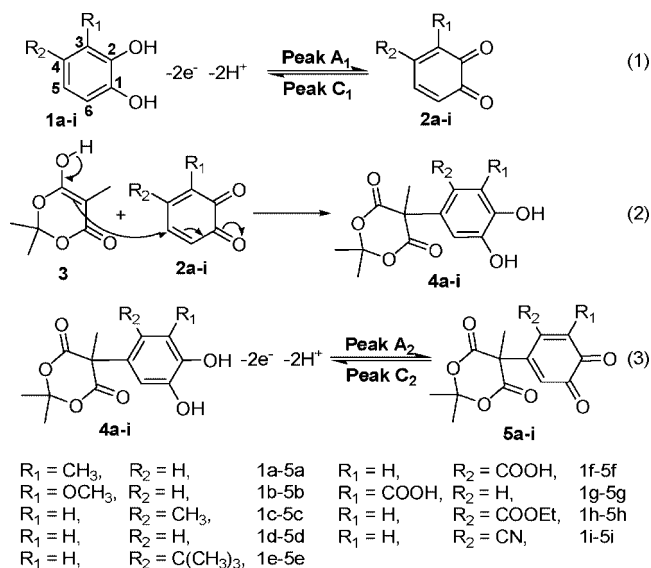
Also, electrochemical oxidation of 3-methylcatechol (**1a**) in the presence of methyl-Meldrum's acid (**3**) was studied at various pH values. The low  $\text{pK}_a$  of methyl-Meldrum's acid (**3**)<sup>25,26</sup> allowed the use of neutral condition (phosphate buffer, pH 7.0, 0.2 M) for electrochemical study of catechols in the presence of methyl-Meldrum's acid (**3**).

Controlled-potential coulometry was performed in aqueous solution (0.2 M phosphate buffer, pH 7.0) containing 0.25 mmol of **1a** and 0.25 mmol of **3** at 0.15 V versus SCE. Cyclic voltammetric analysis carried out during the electrolysis shows the progressive formation of anodic peak A<sub>2</sub>, parallel to the disappearance of peak A<sub>1</sub>. Peak A<sub>1</sub> disappears when the charge consumption becomes about  $2e^-$  per molecule of **1a**. These observations allow us to propose an ECE' pathway in Scheme 1 for the electrochemical oxidation of **1a** in the presence of methyl-Meldrum's acid (**3**). Generation of *o*-benzoquinone **2a** is followed by a Michael addition of **3** to the *o*-benzoquinone **2a**, producing the catechol derivative **4a** as the final product. The oxidation of this compound (**4a**) is more difficult than the oxidation of the parent starting molecule (**1a**) by virtue of the presence of methyl-Meldrum's acid group with electron-withdrawing character on the catechol ring.

According to our results, the anodic peaks of the voltammograms presented in Figure 2 (A<sub>1</sub> and A<sub>2</sub>) pertain to the oxidation of catechols **1a** and **4a** to the *o*-benzoquinones **2a** and **5a**, respectively. Obviously, the cathodic peaks C<sub>1</sub> and C<sub>2</sub> correspond to the reduction of *o*-benzoquinones **2a** and **5a**, respectively.

A scheme for the electrochemical oxidation of catechols in the presence of methyl-Meldrum's acid (**3**) is proposed and tested by digital simulation. On the basis of an ECE' mechanism, the observed homogeneous rate constants ( $k_{\text{obs}}$ ) of reaction of *o*-benzoquinones with methyl-Meldrum's acid (**3**) have been estimated by comparison of the simulation results, (Figure 4 curve b), with experimental cyclic voltammograms (Figure 4

### SCHEME 1



curve a). The transfer coefficient ( $\alpha$ ) was assumed to be 0.5, and the formal potentials were obtained experimentally as the average of the two peak potentials observed in cyclic voltammetry. The heterogeneous rate constants are estimated by use of an experimental working curve.<sup>27</sup>

The procedure is performed based on achieving the best fit between simulated and experimental cyclic voltammograms (Table 1). The method is developed for a variety of scan rates and nucleophile concentrations.

As shown in Table 1, the magnitude of observed homogeneous rate constants ( $k_{\text{obs}}$ ) is dependent on the nature and position of the substituted group on the catechol ring. The presence of electron-donating groups such as methyl (**1a**), methoxy (**1b**), or *tert*-butyl (**1e**) on the catechol ring causes a decrease in  $k_{\text{obs}}$ . In contrast, in the case of **1i** the presence of the nitrile group with electron-withdrawing character causes an increase in  $k_{\text{obs}}$ . In addition, the presence of substituted groups in the C-4 ( $\text{R}_1 = \text{H}, \text{R}_2 \neq \text{H}$ ) position of the catechol ring that is a reactive site of *o*-benzoquinones **2** causes a decrease in the observed homogeneous rate constant ( $k_{\text{obs}}$ ) (Table 1, comparison of **1a** and **1c** or **1f** and **1g**). The observed homogeneous rate

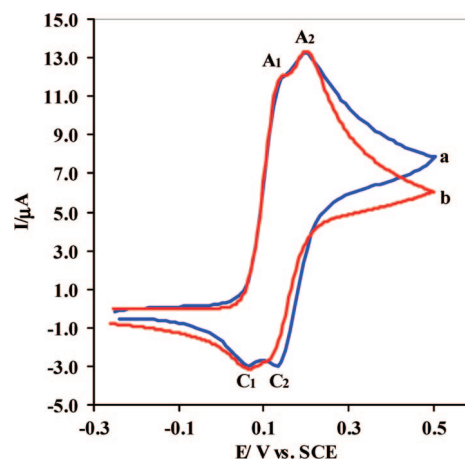


**FIGURE 4.** Cyclic voltammograms of 1.0 mM 3-methylcatechol in phosphate buffer solution (pH 7.0,  $c = 0.2\text{ M}$ ): (a) experimental and (b) simulated. Scan rate: 100  $\text{mV s}^{-1}$ . Working electrode: glassy carbon electrode.  $t = 25 \pm 1^\circ\text{C}$ .

(25) Arnett, E. M.; Maroldo, S. G.; Schilling, S. L.; Harrelson, J. A., Jr. *J. Am. Chem. Soc.* **1984**, *106*, 6759.

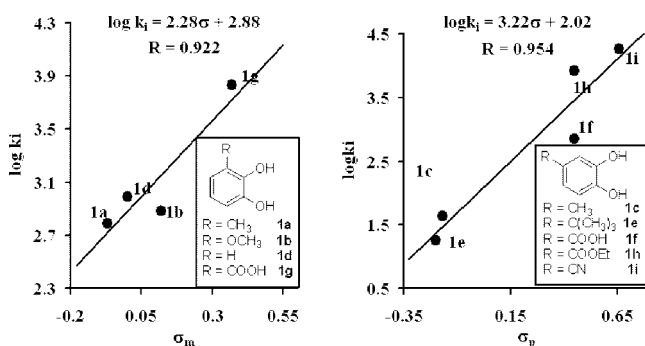
(26) Arnett, E. M.; Harrelson, J. A., Jr. *J. Am. Chem. Soc.* **1987**, *109*, 809.

(27) Greef, R.; Peat, R.; Peter, L. M.; Pletcher, D.; Robinson, J. *Instrumental Methods in Electrochemistry*; Ellis Horwood: Chichester, UK, 1990; p 189.

**TABLE 1.** The Observed Homogeneous Rate Constant ( $k_{\text{obs}}$ ) of the Reaction of Electrochemically Generated *o*-Benzoquinones with Methyl-Meldrum's Acid

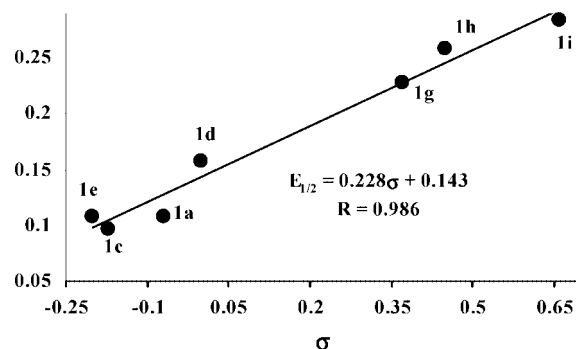
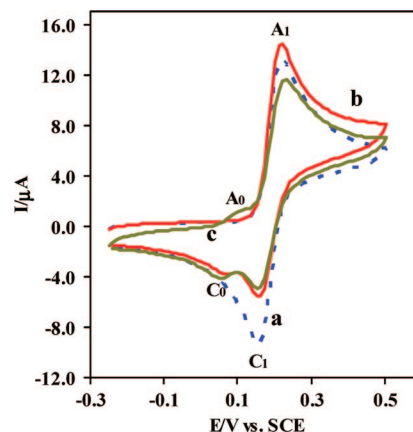
catechols <sup>a</sup>	$E_{1/2}$ vs SCE	electron consumption (mol)	$k_{\text{obs}}$ ( $\text{M}^{-1} \text{s}^{-1}$ ) <sup>b</sup>
1a	0.107	2.1	615 ± 36
1b	0.102	2.2	756 ± 52
1c	0.097	2.1	43 ± 3
1d	0.158	2.3	982 ± 68
1e	0.107	2.1	18 ± 1
1f	0.182	2.2	712 ± 42
1g	0.228	2.4	6800 ± 580
1h	0.258	2.4	8400 ± 621
1i	0.284	2.3	18200 ± 1150

<sup>a</sup>  $R_1 = \text{CH}_3$ ,  $R_2 = \text{H}$  (1a).  $R_1 = \text{OCH}_3$ ,  $R_2 = \text{H}$  (1b).  $R_1 = \text{H}$ ,  $R_2 = \text{CH}_3$  (1c).  $R_1 = \text{H}$ ,  $R_2 = \text{H}$  (1d).  $R_1 = \text{H}$ ,  $R_2 = \text{C}(\text{CH}_3)_3$  (1e).  $R_1 = \text{H}$ ,  $R_2 = -\text{COOH}$  (1f).  $R_1 = -\text{COOH}$ ,  $R_2 = \text{H}$  (1g).  $R_1 = \text{H}$ ,  $R_2 = -\text{COOEt}$  (1h).  $R_1 = \text{H}$ ,  $R_2 = -\text{CN}$  (1i). <sup>b</sup> Standard deviation of four independent simulations at various scan rates.

**FIGURE 5.** Hammett plots for electrochemical oxidation of catechols in the presence of methyl-Meldrum's acid.

constant ( $k_{\text{obs}}$ ) can be related to the Hammett parameters, where the Hammett equation is  $\log k_i = \log k_0 + \sigma\rho$ , where  $k_i$  is the rate constant for substituted catechol,  $k_0$  is the rate constant for catechol,  $\sigma$  is a constant characteristic of a given substituent group,<sup>28</sup> and  $\rho$  is the slope of the  $\log k_i - \sigma$  graph. The Hammett plots are shown in Figure 5. In this figure,  $\sigma_m$  and  $\sigma_p$  are used for C-3 ( $R_2 = \text{H}$ ,  $R_1 \neq \text{H}$ ) and C-4 ( $R_1 = \text{H}$ ,  $R_2 \neq \text{H}$ ) compounds, respectively. The  $\rho$  values in both plots are positive. These positive  $\rho$  values mean that the transition states have substantial negative charge, because the reaction rates are increased significantly for electron-withdrawing substituents.<sup>12,29–33</sup> This result is consistent with the attack of the anion enolate of methyl-Meldrum's acid (3) to the *o*-benzoquinone 2. Also, as shown in Figure 5, the  $\rho$  value for C-4 ( $R_1 = \text{H}$ ,  $R_2 \neq \text{H}$ )-substituted catechols (3.22) is greater than that for C-3 ( $R_2 = \text{H}$ ,  $R_1 \neq \text{H}$ )-substituted catechols (2.28). This means that the effect of substituents on C-4-substituted catechols is much larger than that on the C-3-substituted catechols.

Also, the half-wave potential ( $E_{1/2}$ ) of catechols is quite sensitive to substituent effects as is shown in Table 1. A plot of  $E_{1/2}$  versus  $\sigma$  confirms the sensitivity of  $E_{1/2}$  to the characteristic of the substituent group (Figure 6). The positive

 $E_{1/2}$  V vs. SCE**FIGURE 6.**  $E_{1/2} - \sigma$  plot for catechols.**FIGURE 7.** Cyclic voltammograms of 1.0 mM 3,4-dihydroxybenzoic acid: (a) in the absence and (b and c) first and second scan in the presence of 1.0 mM Meldrum's acid at a glassy carbon electrode, in phosphate buffer solution (pH 7.0,  $c = 0.2 \text{ M}$ ). Scan rate:  $100 \text{ mV s}^{-1}$ .  $t = 25 \text{ }^\circ\text{C}$ .

slope value means that the  $E_{1/2}$  is increased significantly for electron-withdrawing substituents.<sup>34–38</sup>

**Electrochemical Oxidation of 4-Substituted Catechols in the Presence of Meldrum's Acid.** As in the previous case, voltammetric experiments were carried out in aqueous phosphate buffer solution (pH 7.0,  $c = 0.2 \text{ M}$ ). Figure 7 (curve a) shows a typical voltammetric curve for a 1.0 mM solution of 3,4-dihydroxybenzoic acid (1f). One anodic peak ( $A_1$ ) and the related cathodic peak ( $C_1$ ) which corresponds to the transformation of 1f to *o*-benzoquinone 2f and vice versa within a quasireversible two-electron process<sup>39,40</sup> are observed. The oxidation of 1f in the presence of Meldrum's acid (3a) as a nucleophile was studied in some detail. Figure 7 (curve b) shows the cyclic voltammogram obtained for a 1.0 mM solution of 1f in the presence of Meldrum's acid (3a). In this condition, the voltammogram exhibits one anodic peak ( $A_1$ ) and two cathodic peaks ( $C_1$  and  $C_0$ ). The second cyclic voltammogram shows that one new anodic peak  $A_0$  appears at less positive potentials.

Furthermore, it is seen that proportional to the increase of potential sweep rate, parallel to the increase in height of the

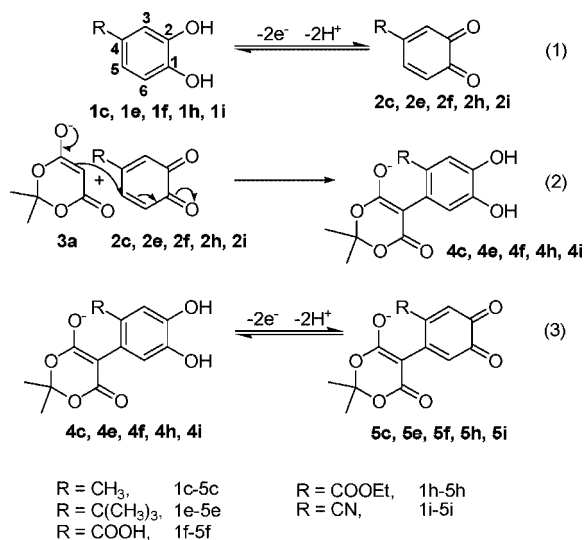
(28) Hansch, C.; Leo, A.; Taft, R. W. *Chem. Rev.* **1991**, *91*, 165.  
 (29) Job, D.; Dunford, H. B. *Eur. J. Biochem.* **1976**, *66*, 607.  
 (30) Saleem, M. M. M.; Wilson, M. T. *Biochem. J.* **1982**, *201*, 433.  
 (31) Nematollahi, D.; Alimoradi, M.; Waqif Husain, S. *Electroanalysis* **2004**, *16*, 1359.  
 (32) Nematollahi, D.; Ariapad, A.; Rafiee, M. *J. Electroanal. Chem.* **2007**, *602*, 37.  
 (33) Nematollahi, D.; Mazloum Ardekani, M.; Shekarlab, N. *Int. J. Chem. Kinet.* **2007**, *39*, 605.

(34) Zuman, P. *Substituents Effects in Organic Polarography*; Plenum Press: New York, 1967.  
 (35) Qureshi, G. A.; Ireland, N. *Bull. Soc. Chim. Belg.* **1981**, *90*, 223.  
 (36) Li, C. Y.; Caspar, M. L.; Dixon, D. W. *Electrochim. Acta* **1980**, *25*, 1135.  
 (37) Huntington, J. L.; Davis, D. G. *J. Electrochem. Soc.* **1971**, *118*, 57.  
 (38) Stradins, J.; Glezer, V.; Turovska, B.; Markava, E.; Freimanis, J. *Electrochim. Acta* **1991**, *36*, 1219.  
 (39) Nematollahi, D.; Goodarzi, H. *J. Org. Chem.* **2002**, *67*, 5036.  
 (40) Nematollahi, D.; Rafiee, M. *Green Chem.* **2005**, *7*, 638.

**TABLE 2.** Experimental and Simulated Parameters for Catechols in the Presence of Meldrum's Acid

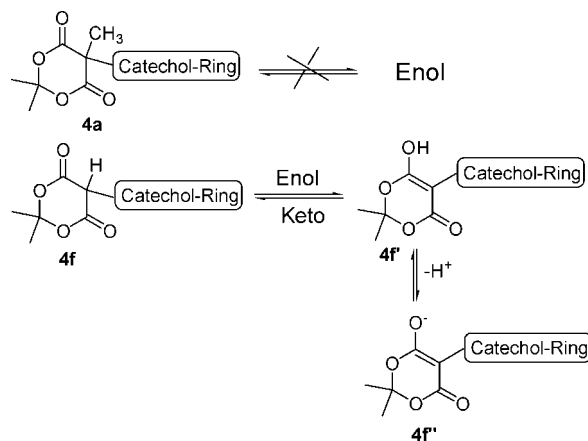
catechol <sup>a</sup>	electron consumption (mol)	$k_{\text{obs}}$ ( $\text{M}^{-1} \text{s}^{-1}$ ) <sup>b</sup>
<b>1a</b>	6.05	151 ± 9
<b>1b</b>	6.09	195 ± 13
<b>1c</b>	4.02	20.3 ± 1
<b>1d</b>	6.03	225 ± 10
<b>1e</b>	4.06	5.7 ± 0.3
<b>1f</b>	4.10	173 ± 13
<b>1g</b>	6.15	1500 ± 90
<b>1h</b>	4.11	2100 ± 189
<b>1i</b>	4.12	6000 ± 480

<sup>a</sup> **1c**, **1e**, **1f**, **1h**, and **1i** have been simulated according to the ECE mechanism. **1a**, **1b**, **1d**, and **1g** have been simulated according to the ECECE mechanism. <sup>b</sup> Standard deviation of four independent simulations at various scan rates.

**SCHEME 2**

$C_1$ , the height of  $C_0$  decreases. A similar situation is observed when the Meldrum's acid (**3a**) to **1f** concentration ratio is decreased. A plot of the peak current ratio ( $I_{\text{PC1}}/I_{\text{PA1}}$ ) versus scan rate for a mixture of 3,4-dihydroxybenzoic acid (**1f**) and Meldrum's acid (**3a**) confirms the reactivity of **2f** toward Meldrum's acid (**3a**), appearing as an increase in the peak current ratio ( $I_{\text{PC1}}/I_{\text{PA1}}$ ) at higher scan rates. On the other hand, the current function for peak  $A_1$  ( $I_{\text{PA1}}/\nu^{1/2}$ ) decreases with an increase in the scan rate.

Controlled-potential coulometry was performed in aqueous solution (phosphate buffer,  $c = 0.2 \text{ M}$ , pH 7.0) containing 0.30 mmol of 3,4-dihydroxybenzoic acid (**1f**) and 0.30 mmol of **3a** at peak  $A_1$  potential. Cyclic voltammetric analysis carried out during the electrolysis shows the progressive formation of a new anodic peak ( $A_0$ ), parallel to the disappearance of peak  $A_1$ . The anodic peak  $A_1$  and cathodic peak  $C_1$  disappear when the charge consumption becomes about  $4e^-$  per molecule of **1f** (Table 2). Contrary to the previous case, these observations are indicative of an ECE (Electron transfer–Chemical reaction–Electron transfer) mechanism and allows the proposal of the pathway for the electrooxidation of 3,4-dihydroxybenzoic acid (**1f**) in the presence of Meldrum's acid (**3a**) (Scheme 2). Accordingly, the 1,4-addition (Michael) reaction of **3a** to the *o*-benzoquinone **2f** leads to intermediate **4f**. The oxidation of **4f** is easier than the oxidation of **1f** by virtue of the presence of

**SCHEME 3**

Meldrum's acid group with electron-donating (contrary to methyl-Meldrum's acid) character on the catechol ring.

According to our results, the anodic peaks  $A_1$  and  $A_0$  pertain to the oxidation of catechols **1f** and **4f** to the *o*-benzoquinones **2f** and **5f**, respectively. Obviously, the cathodic peaks  $C_1$  and  $C_0$  correspond to the reduction of *o*-benzoquinones **2f** and **5f**, respectively.

The most important difference between this case and the previous case is the number of transferred electrons during controlled-potential coulometry. Contrary to the previous case, the results show that the consumed charge is about  $4e^-$  per molecule of 3,4-dihydroxybenzoic acid (**1f**). This is related to the electron-donating character of Meldrum's acid (in intermediate **4f**) (Scheme 3), in comparison with the electron-withdrawing character of methyl-Meldrum's acid (in intermediate **4a**) giving rise to the presence of two acidic protons in **4f** (Figure 1) or one acidic proton in intermediate **4f** (Scheme 3).

As shown in Scheme 3, contrary to **4a**, intermediate **4f** can be converted to anion enolate **4f'**. This transformation caused that Meldrum's acid (**3a**) to act as an electron-donating substituent.

On the basis of an ECE mechanism, the observed homogeneous rate constants ( $k_{\text{obs}}$ ) of the reaction of *o*-benzoquinones **2c**, **2e**, **2f**, **2h**, and **2i** with Meldrum's acid (**3a**) have been estimated by comparison of the simulation results, with experimental cyclic voltammograms, under the above-mentioned conditions (Table 2). The procedure is performed based on achieving the best fit between simulated and experimental cyclic voltammograms.

**Electrochemical Oxidation of 3-Substituted Catechols in the Presence of Meldrum's Acid.** Cyclic voltammograms recorded for 1.0 mM 2,3-dihydroxybenzoic acid (**1g**) in aqueous solutions show an anodic peak ( $A_1$ ) and a cathodic counterpart peak ( $C_1$ ) which corresponds to the transformation of **1g** to *o*-benzoquinone **2g** and vice versa within a quasireversible two-electron process.<sup>39,40</sup> The oxidation of **1g** in the presence of Meldrum's acid (**3a**) was studied in some detail. Figure 8 shows the cyclic voltammogram obtained for a 1.0 mM solution of **1g** in the presence of Meldrum's acid (**3a**) in aqueous solution containing 0.2 M phosphate buffer (pH 7.0). In this condition, the voltammogram exhibits one anodic peak ( $A_1$ ) and three cathodic peaks ( $C_1$ ,  $C_0$ , and  $C_{00}$ ). The second cyclic voltammogram shows that two new anodic peaks  $A_0$  and  $A_{00}$  appear at less positive potentials.

Also, it is seen that proportional to the augmentation of potential sweep rate, parallel to the increase in height of the

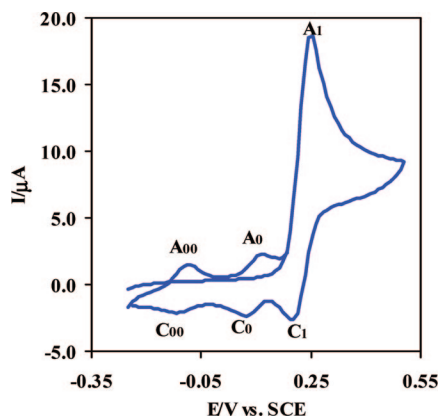


**FIGURE 8.** Cyclic voltammograms (first and second scans) of 1.0 mM 2,3-dihydroxybenzoic acid (**1g**) in the presence of 1.0 mM Meldrum's acid (**3a**) at a glassy carbon electrode, in phosphate buffer solution (pH 7.0,  $c = 0.2$  M). Scan rate:  $100 \text{ mV s}^{-1}$ .  $t = 25^\circ\text{C}$ .

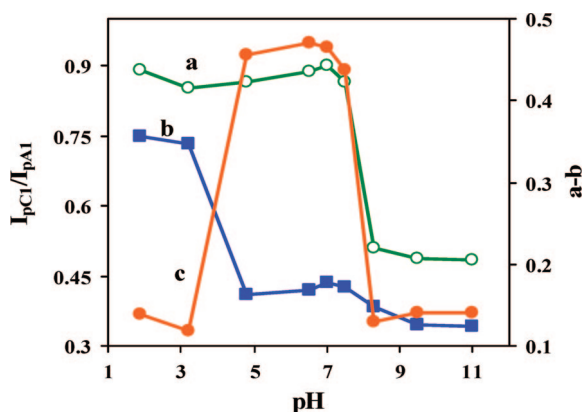


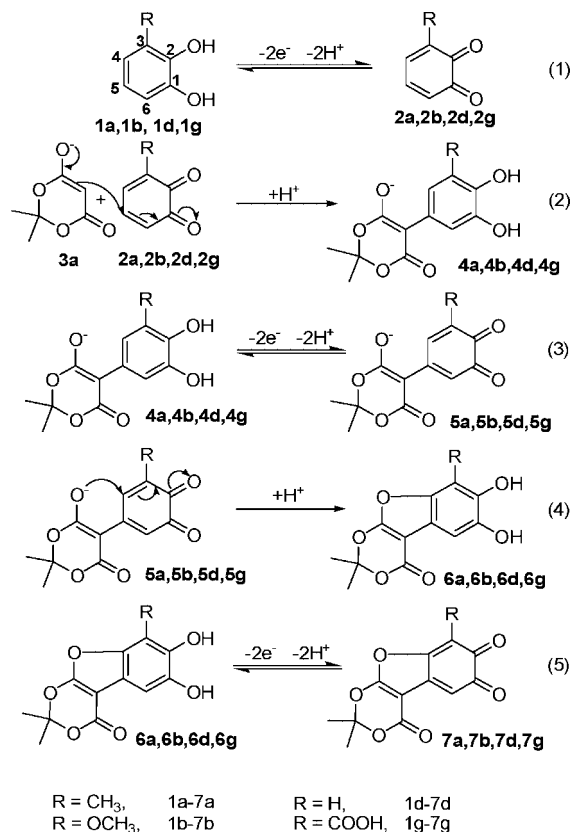
**FIGURE 9.** Variation of peak current ratio ( $I_{pC1}/I_{pA1}$ ) of 2,3-dihydroxybenzoic acid versus pH (a) in the absence of Meldrum's acid, (b) in the presence of Meldrum's acid, and (c) the difference between peak current ratio ( $I_{pC1}/I_{pA1}$ ) in the presence and absence of Meldrum's acid (curve a – curve b).

$C_1$ , the heights of  $C_0$  and  $C_{00}$  decrease. A similar situation is observed when the **3a** to **1g** concentration ratio is decreased. A plot of peak current ratio ( $I_{pC1}/I_{pA1}$ ) versus scan rate for a mixture of **1g** and **3a**, appearing as an increase in the peak current ratio ( $I_{pC1}/I_{pA1}$ ) at higher scan rates, confirms the reactivity of **2g** toward **3a**. On the other hand, the current function for peak  $A_1$  ( $I_{pA1}/v^{1/2}$ ) decreases with an increase in the scan rate.

In addition, electrochemical oxidation of **1g** in the presence of Meldrum's acid (**3a**) ( $pK_a = 4.97$ )<sup>41</sup> was studied at various pH values (Figure 9, curve b). The results indicate that the peak current ratio ( $I_{pC1}/I_{pA1}$ ) increases with decreasing pH. This can be related to protonation of Meldrum's acid (**3a**) and inactivation of it toward the Michael addition reaction with *o*-benzoquinone **2g**. This indicates that the rate of the coupling reaction is pH dependent and enhanced by increasing pH in the range of 5–7. In this range, the difference between the peak current ratio ( $I_{pC1}/I_{pA1}$ ) in the presence (curve b) and absence of Meldrum's acid (**3a**) (curve a) is maximum (curve c). In this study, a solution containing phosphate buffer (pH 7.0,  $c = 0.2$  M) has been selected for electrochemical study of catechols in the presence of Meldrum's acid (**3a**).

Controlled-potential coulometry was performed in aqueous solution ( $c = 0.2$  M phosphate buffer, pH 7.0) containing 0.25

## SCHEME 4



mmol of **1g** and 0.25 mmol of Meldrum's acid (**3a**) at 0.25 V (versus SCE). The monitoring of electrolysis progress was carried out by cyclic voltammetry. It shows that proportional to the advancement of coulometry, the anodic peak  $A_1$  decreases and disappears when the charge consumption becomes about  $6e^-$  per molecule of **1g**. Coulometric results for various catechols have been shown in Table 2.

These observations allow us to propose an ECECE mechanism for electrochemical oxidation of 2,3-dihydroxybenzoic acid (**1g**) and other C-3-substituted catechols in the presence of Meldrum's acid (**3a**) (Scheme 4).

According to our results, it seems that the Michael addition reaction of the anion enolate of **3a** to *o*-benzoquinone **2g** (eq 2) is faster than other side reactions and leads to intermediate **4g**. The oxidation of compound **4g** is easier than the oxidation of parent-starting molecule **1g** by virtue of the presence of an electron-donating group (eq 3). In the next step, *o*-benzoquinone **5g**, via an intramolecular Michael reaction, is converted to intermediate **6g** (eq 4). Further oxidation converts intermediate **6g** into the final product **7g**. Also, according to our results, the anodic peaks  $A_1$ ,  $A_0$ , and  $A_{00}$  pertain to the oxidation of catechols **1g**, **4g**, and **6g** to the *o*-benzoquinone **2g**, **5g**, and **7g**, respectively. Obviously, the cathodic peaks  $C_1$ ,  $C_0$ , and  $C_{00}$  correspond to the reduction of *o*-benzoquinones **2g**, **5g**, and **7g**, respectively.

The electrochemical oxidation of catechols in the presence of Meldrum's acid is proposed and tested by digital simulation. On the basis of an ECECE mechanism, the observed homogeneous rate constants ( $k_{\text{obs}}$ ) of the reaction of *o*-benzoquinones **2a**, **2b**, **2d**, and **2g** with Meldrum's acid have been estimated by comparison of the simulation results, with experimental cyclic voltammograms. The calculated homogeneous rate constants are

(41) Pihlaja, K.; Seilo, M. *Acta Chem. Scand.* **1969**, *23*, 3003.

given in Table 2. As shown in Table 2 and as discussed before, the magnitude of the observed homogeneous rate constant ( $k_{\text{obs}}$ ) is dependent on the nature and position of the substituted group on the catechol ring. In this study, because of the electron-donating and steric characters of the *tert*-butyl group and its presence in the C-4 position of the catechol ring, the least observed homogeneous rate constant ( $k_{\text{obs}}$ ) belongs to 4-*tert*-butylcatechol. A comparison of the observed homogeneous rate constants ( $k_{\text{obs}}$ ) of Tables 1 and 2 has revealed that  $k_{\text{obs}}$  for the reaction of anion enolate of methyl-Meldrum's acid (**3**) with *o*-quinones **2a–i** is greater than  $k_{\text{obs}}$  for reaction of anion enolate of Meldrum's acid (**3a**). This can be related to the higher reactivity of the anion enolate of methyl-Meldrum's acid (**3**) in comparison with the anion enolate of Meldrum's acid (**3a**).

## Experimental Section

**Apparatus and Reagents.** Reaction equipment is described in the Supporting Information. The homogeneous rate constants were estimated by analyzing the cyclic voltammetric responses, using the DigiElch simulation software.<sup>42</sup> An excellent fit between the experimental and simulated data was obtained over this range of experimental conditions for the following kinetic parameter values.

All chemicals (catechols, methyl-Meldrum's acid, and Meldrum's acid) were reagent-grade materials, and phosphate salts were of pro-analysis grade. These chemicals were used without further purification.

**Electroorganic Synthesis of 4a–c.** In a typical procedure, 80 mL of solution containing 0.2 M phosphate buffer (pH 7.0) was pre-electrolyzed at 0.20 V vs SCE, in an undivided cell; then 2 mmol of catechol (**1a–c**) and methyl-Meldrum's acid (**3**) (2 mmol) were added to the cell. The electrolysis was terminated when the decay of the current became more than 95%. The process was interrupted during the electrolysis and the graphite anode was washed in acetone to reactivate it. At the end of electrolysis, a few drops of phosphoric acid were added to the solution and the cell was placed in the refrigerator overnight. The precipitated solid was collected by filtration and washed with water. After washing, products were characterized by IR, <sup>1</sup>H NMR, <sup>13</sup>C NMR, and MS. The isolated yields of **4a–c** are 66%, 49%, and 40%, respectively.

**Characteristic of Products. Compound 4a:** mp 260–262 °C dec; IR<sub>(KBr)</sub> 3432, 3350, 2991, 2936, 1767, 1715, 1618, 1603, 1528, 1498, 1432, 1395, 1376, 1307, 1257, 1204, 1161, 1107, 1074, 1030, 997, 978, 936, 902, 874, 840, 740, 716, 699, 624, 602 cm<sup>-1</sup>; <sup>1</sup>H NMR,  $\delta$  (90 MHz acetone-*d*<sub>6</sub>) 1.26 (s, 3H), 1.62 (s, 3H), 1.66 (s, 3H), 2.16 (s, 3H), 6.57 (d, 1H), 6.67 (d, 1H), 7.35 (br), 8.61 (br); <sup>13</sup>C NMR (90 MHz, CDCl<sub>3</sub>)  $\delta$  15.7, 26.1, 27.1, 29.4, 55.0, 106.1, 110.1, 119.9, 125.0, 127.7, 143.4, 144.0, 168.3; MS *m/e* (rel intensity) 280 (46), 178 (61), 167 (26), 150 (100), 43 (35).

**Compound 4b:** mp 281–283 °C dec; IR<sub>(KBr)</sub> 3467, 3000, 2944, 1775, 1740, 1673, 1633, 1614, 1515, 1453, 1431, 1379, 1240, 1206,

1104, 997, 977, 936, 901, 867, 844, 699, 623 cm<sup>-1</sup>; <sup>1</sup>H NMR (90 MHz DMSO-*d*<sub>6</sub>)  $\delta$  1.63 (s, 3H), 1.82 (s, 3H), 1.97 (s, 3H), 3.40 (s, 3H), 6.55 (s, 1H), 6.84 (s, 1H), 8.94 (br).

**Compound 4c:** mp 257–259 °C dec; IR<sub>(KBr)</sub> 3433, 3000, 2952, 1764, 1725, 1698, 1609, 1526, 1510, 1456, 1399, 1383, 1280, 1241, 1201, 1160, 1134, 1064, 1016, 980, 901, 869, 857, 845, 802, 752, 724, 661, 616, 582 cm<sup>-1</sup>; <sup>1</sup>H NMR (90 MHz DMSO-*d*<sub>6</sub>)  $\delta$  1.56 (s, 3H), 1.76 (s, 3H), 1.82 (s, 3H), 2.01 (s, 3H), 6.58 (s, 1H), 6.88 (s, 1H), 7.92 (br). <sup>13</sup>C NMR,  $\delta$  (90 MHz acetone-*d*<sub>6</sub>): 18.9, 23.3, 27.5, 28.9, 51.7, 106.1, 115.3, 119.2, 125.5, 127.2, 143.3, 144.9, 168.1.

## Conclusion

We have investigated the use of the electrochemistry for the synthesis of some new catechol derivatives (**4a–c**) by oxidation of catechols **1a–c** in the presence of methyl-Meldrum's acid (**3**) in aqueous solutions. The overall reaction mechanism for anodic oxidation of catechols, in the presence of methyl-Meldrum's acid (**3**), is presented in Scheme 1. The kinetics of the reaction of electrochemically generated *o*-benzoquinones with the methyl-Meldrum's acid (**3**) is studied by the cyclic voltammetry and the simulation of obtained voltammograms under the ECE' mechanism. Also, the effects of the substituted groups on the catechol ring in  $k_{\text{obs}}$  (Hammett plot) have been studied. In addition, the reaction of electrochemically generated *o*-benzoquinones **2a–i** with Meldrum's acid (**3a**) has been studied. Contrary to the previous case, the results indicate that the reaction mechanism is ECE and ECECE in the case of C-4 and C-3 catechols, respectively. The overall reaction mechanisms for anodic oxidation of catechols (**1a–i**) in the presence of Meldrum's acid (**3a**) are presented in Schemes 2 and 4. Also, based on ECE and ECECE mechanisms, the homogeneous rate constants were estimated by comparing the experimental cyclic voltammetric responses with the digital simulated results. There is good agreement between the simulated voltammograms and those obtained experimentally. Furthermore, the effect of nucleophile on the oxidation pathway of catechols has been discussed.

**Acknowledgment.** We would like to thank Dr. M. Rudolph for his cyclic voltammogram digital simulation software (DigiElch SB) and the authors acknowledge the Bu-Ali Sina University Research Council and Center of Excellence in Development of Chemical Methods (CEDCM) for support this work.

**Supporting Information Available:** Copies of <sup>1</sup>H, <sup>13</sup>C NMR, FT-IR and MS of all compounds (**4a–c**), as well as cyclic voltammograms of **1f** and **1g** in the presence of Meldrum's acid in various scan rates, and during controlled potential coulometry (in the case of **1g**). This material is available free of charge via the Internet at <http://pubs.acs.org>.

JO800115N

(42) (a) Rudolph, M. J. *Electroanal. Chem.* **2002**, 529, 97. (b) Also, see: <http://www.digielch.de>.